Nuclear Instruments and Methods in Physics Research B 350 (2015) 41–48

Contents lists available at ScienceDirect

Nuclear Instruments and Methods in Physics Research B

journal homepage: www.elsevier.com/locate/nimb

Validation of the GEANT4 simulation of bremsstrahlung from thick targets below 3 MeV

L. Pandola [a,b,*], C. Andenna [c], B. Caccia [d]

[a] INFN, Laboratori Nazionali del Sud, Via Santa Sofia 62, I-95125 Catania, Italy
[b] INFN, Gran Sasso Science Institute, Viale Francesco Crispi 7, I-67100 L'Aquila, Italy
[c] INAIL, Dipartimento Innovazioni Tecnologiche e Sicurezza degli Impianti, Prodotti ed Insediamenti Antropici, Via Alessandria 220, I-00198 Roma, Italy
[d] Dipartimento Tecnologie e Salute, Istituto Superiore di Sanità and INFN, Gruppo Collegato dell'Istituto Superiore di Sanità, Viale Regina Elena 299, I-00161 Roma, Italy

ARTICLE INFO

Article history:
Received 8 October 2014
Received in revised form 11 March 2015
Accepted 11 March 2015
Available online 27 March 2015

Keywords:
Monte Carlo simulations
Bremsstrahlung
Medical physics

ABSTRACT

The bremsstrahlung spectra produced by electrons impinging on thick targets are simulated using the GEANT4 Monte Carlo toolkit. Simulations are validated against experimental data available in literature for a range of energy between 0.5 and 2.8 MeV for Al and Fe targets and for a value of energy of 70 keV for Al, Ag, W and Pb targets. The energy spectra for the different configurations of emission angles, energies and targets are considered. Simulations are performed by using the three alternative sets of electromagnetic models that are available in GEANT4 to describe bremsstrahlung.

At higher energies (0.5–2.8 MeV) of the impinging electrons on Al and Fe targets, GEANT4 is able to reproduce the spectral shapes and the integral photon emission in the forward direction. The agreement is within 10–30%, depending on energy, emission angle and target material. The physics model based on the Penelope Monte Carlo code is in slightly better agreement with the measured data than the other two. However, all models over-estimate the photon emission in the backward hemisphere. For the lower energy study (70 keV), which includes higher-Z targets, all models systematically under-estimate the total photon yield, providing agreement between 10% and 50%.

The results of this work are of potential interest for medical physics applications, where knowledge of the energy spectra and angular distributions of photons is needed for accurate dose calculations with Monte Carlo and other fluence-based methods.

1. Introduction

The need for the precise description of the photon emission by electron bremsstrahlung in thick targets is common to many fields of research, including medical physics, astrophysics and astroparticle physics. While bremsstrahlung starts to dominate over ionization for energies of tens of MeV, the process may be relevant and measurable also at much lower energies, because of the longer mean free path of photons with respect to electrons.

The simulation of the bremsstrahlung emission is especially relevant in medical physics applications, where the clinical X-ray beams are produced by electrons of kinetic energies between 10 keV and 50 MeV decelerated in metallic targets. A fraction of the electrons kinetic energy is transformed in the target into heat, and a fraction of the energy is emitted in the form of bremsstrahlung photons. The knowledge of the energy spectrum and angular distribution of photon beams produced in the interaction is essential for accurate dose calculations in the patient and represents the most rigorous description of beam quality [1]. In external radiotherapy, to optimize the dose distribution in a patient, the beam is modulated in intensity and shape. The radiation treatment outcome is related to the accuracy in the delivered dose to the patient that depends on the accuracy of beam data [2] and quality assurance procedures [3,4]. The quality assurance program for linear accelerators requires that the machine characteristics do not deviate significantly from their baseline values acquired at the time of acceptance and commissioning [3,4]. The main reason for the requirement of high accuracy in dose delivery is typically the narrow margin between the dose needed for tumor control and the dose causing complications for healthy tissues. Targets in clinical linear accelerators are thick enough to stop the primary electrons completely. Due to the interplay with other concurrent physical processes which can affect the kinetic energy and the direction of the electrons in thick media, it is very difficult to

* Corresponding author at: INFN, Laboratori Nazionali del Sud, Via Santa Sofia 62, I-95125 Catania, Italy.
E-mail address: pandola@lns.infn.it (L. Pandola).

http://dx.doi.org/10.1016/j.nimb.2015.03.033
0168-583X/

obtain the spectral and angular photon distributions using analytical methods such as the Schiff theory [5,6]. Calculations must hence be performed by using Monte Carlo simulations. Many different codes are available for this purpose, including Geant4 [7,8], Penelope [9], EGSNRC [10] and Fluka [11,12].

The aim of this work is the validation of the bremsstrahlung emission (total radiated energy and energy/angular spectra) in thick targets as predicted by Geant4, tailored to the requirements and the applications that are typical of medical physics. Since the region between 15 and 30 MeV was already considered by other authors [13], a special focus is given to lower energies. Suitable experimental measurements of bremsstrahlung emission in thick targets at such low energies are not readily found in the literature. Two sets of measurements are considered for this work:

1. Dance et al. [14], which reports absolute energy and angular double-differential photon spectra for electron energies between 0.5 and 2.8 MeV in aluminum and iron thick targets;
2. Ambrose et al. [15], which displays absolute energy spectra for 70 keV electrons impinging at two different angles on thick targets of aluminum, silver, tungsten and lead.[1]

The work presented here is not meant to be a comprehensive or a quantitative validation of the Monte Carlo simulation, as done in other papers in the recent literature [16–19]. The main goal is to give a general overview of the physics performance of Geant4 in this domain as well as to clearly indicate the regimes where measurement and simulation disagree, which may be relevant to the users of the code.

The paper is organized as follows: in Section 2 the Geant4-based Monte Carlo simulation which was developed to reproduce the reference experimental data is described. An overview is given of the alternative physics models that are presently available in Geant4 to describe bremsstrahlung in the energy range of interest. The outcome and the results provided by the simulation are shown and reported in Section 3; the agreement with the reference data is discussed in detail and strong and weak points of the simulations are emphasized. General conclusions about the validity and reliability of Geant4-based simulations concerning the production of bremsstrahlung photons are drawn in Section 4, with a focus on medical applications.

2. The Monte Carlo simulation with Geant4

As mentioned above, data from Refs. [14,15] were used in this work to validate the physics results provided by the Geant4 code. Geant4 [7,8] is a general-purpose toolkit for the Monte Carlo simulation of the propagation of particles in matter. It includes a variety of physics models to describe the electromagnetic and hadronic interactions of many kinds of particles, including γ-rays, leptons, baryons, mesons and nuclei. The comparison work presented in this paper has been carried out with the version 9.6.p02 of Geant4 (May, 2013). While a more recent version of Geant4 was made available in the meanwhile (10.0, December, 2013), no changes are reported in the release notes for the physics models that are relevant for the simulation of bremsstrahlung photons at low energy.

2.1. Geant4 physics models

Three independent sets of electromagnetic models are available in Geant4 that are appropriate to simulate bremsstrahlung in the energy range considered in this work: "Standard" [7,20–23], "Livermore" [22–24] and Penelope [9,21,23]. The constructors available in Geant4 can be used to register all electromagnetic processes in the user application. In the case of the Standard package the so-called "Option3" (`G4EmStandardPhysics_option3`) is used which is tailored to medical and space application [21]. For Livermore and Penelope the constructors `G4EmLivermorePhysics` and `G4EmPenelopePhysics` are used, respectively. All model parameters are unchanged with respect to the default provided in Geant4 9.6.p02.

In the Geant4 unified scheme for the electromagnetic physics, different models can be used for the same physics process. The process which is devoted to describe the bremsstrahlung of electrons and positrons is `G4eBremsstrahlung`. The bremsstrahlung models used by `G4eBremsstrahlung` for the physics lists used in this work are: `G4SeltzerBergerModel` in Option3,[2] `G4LivermoreBremsstrahlungModel` in "Livermore" and `G4PenelopeBremsstrahlungModel` in "Penelope".

The cross sections used by the model `G4SeltzerBergerModel` are based on the interpolation of published tables [25,26], which account for the bremsstrahlung emission in the field of nuclei and of atomic electrons. The published tables contain energy-differential cross sections $d\sigma/dE$ between 1 keV and 10 GeV. The uncertainty reported in the original work for the energy range of interest of this work is "about 10%" below 2 MeV and "between 5% and 10%" between 2 and 50 MeV [26]. The integral cross section is calculated numerically from the differential tables at the initialization of Geant4. The angular distribution, following the successful sampling of the radiated energy, is calculated according to a simplified version of the Tsai's formula [27,28], as described in Ref. [29]. The simplified formula is appropriate for very high energies, but is expected to be much less accurate in the MeV range.

The total cross section used by the model `G4LivermoreBremsstrahlungModel` is obtained from the interpolation of the evaluated cross section data from the EEDL Livermore library [30]. The shape of the photon energy spectra is also derived by interpolation of the data reported from the EEDL library. Values are listed as a function of the ratio κ between the photon energy k and the electron energy T_0: the tabulated data set contains 15 points for each element ranging between $\kappa = 0.01$ and $\kappa = 1$, and a linear interpolation method is used. The angular distribution is sampled according to 2BS formula by Koch and Motz [5], using the algorithm developed by Bielajew [31] and implemented in EGS4. The 2BN formula by Koch and Motz [5] and a simplified version of the Tsai distribution [27] are also available as alternative options. In the present work, only the 2BS default generator was considered.

The model `G4PenelopeBremsstrahlungModel` is the re-engineering in Geant4 of the bremsstrahlung model of Penelope Monte Carlo code v2008 [9,32,33]. The total cross sections that are used for the evaluation of the restricted cross sections above the production threshold are taken from the EEDL Livermore library. The shape of the photon emission spectra are sampled according to a parametrization of the data reported in the tables of Ref. [26]. Data are available for all elements; the grid has 57 electron energies between 1 keV and 10 GeV and 32 points in the photon energy $\kappa = k/T_0$ between 10^{-12} and 1. A log–log interpolation is performed between the grid points. The angular distribution is sampled from a modified Lorentz distribution [9,33], whose parameters are fitted to match the shape functions reported by Kissel [34] for the following benchmark cases: $Z = 2$, 8, 13, 47, 79 and 92; $E = 1$, 5, 10, 50, 100 and 500 keV; $\kappa = 0$, 0.6, 0.8 and 1.0.

[1] Measurements in others materials were also taken ("for a range of Z from 6 to 92"). However, they are not reported or shown individually in the paper and are hence not usable for validation purposes.

[2] For electrons and positrons above 1 GeV, a specific relativistic model `G4eBremsstrahlungRelModel` is used. Given the energy range of interest, this is not relevant for the present work, and actually never invoked.

The abstract interface `G4VEmAngularGenerator` provides the possibility of using for each model an alternative angular generator than the default one. For instance, the angular generator `G4PenelopeBremsstrahlungAngular` which implements the sampling according to the modified Lorentz dipole distribution can be also registered to the other models.

2.2. The user application

A dedicated user application was developed to simulate the passage of electrons in a thick target, and to score energy and direction of all photons leaving the target. All relevant physics processes were considered by using the GEANT4 constructors described in Section 2.1. Therefore, the simulation properly accounts for the slow-down of the electrons due to ionization and for the possible back-scattering from the target. The energy T_0 of the impinging electrons, the thickness and the material of the target can be changed at run-time by means of a user interface. In the simulation jobs for Dance et al. the cut-in-range for the production of secondary photons and electrons was set to 2.5 μm, which is much smaller than the thickness of the targets (between 0.32 and 6.4 mm in the various configurations). The minimum photon energy which is allowed by the cuts was 250 eV in both Al and Fe, which is below the energy of the characteristic X-rays. The cut values are also well below the experimental energy threshold reported in Dance et al. [14], which is between 46 and 171 keV. Such a cut was found to be the optimal trade-off between CPU performances and tracking precision in the target. In the simulation jobs for Ambrose et al. the production cut-in-range is 1 μm, while the thickness of the target is between 18 and 94 μm. Also in this case, the threshold used in the simulation was low enough to allow the production of fluorescence X-rays in all target materials.

Simulations were run on different Linux machines, in which GEANT4 had been built and compiled from the source code. At least 10^9 primary electrons were generated for each of the eight configurations reported by Dance et al., i.e. four energies (T_0 = 0.5, 1.0, 2.0 and 2.8 MeV) and two target materials (Al and Fe), and for the four configurations reported by Ambrose et al. (i.e. Al, Ag, W and Pb). Primary electrons were assumed to form an ideally monochromatic pencil beam. Simulations were then run for the three sets of GEANT4 physics models described in Section 2.1. The CPU time required to get comparable statistical precision in the simulation outputs was typically between 8 and 24 h for each specific configuration. Time differences are mostly related to the target thickness, than to the physical models considered: for a given configuration, the Penelope and Livermore simulations take 15–20% longer than Option3.

3. Comparison with experimental data: results and discussion

The papers that were selected as the reference for this study do not provide tabulated data: measurements are displayed in graphical form only. No assessment of experimental uncertainties is available from Ambrose et al. The uncertainty of each data point in the double differential spectra by Dance et al. is evaluated by the authors to be between 15% and 18%. The uncertainty due to the digitization procedure is much smaller (<5%), so that the global uncertainty considered here for the digitized data points is 20%. The uncertainty of the integrated radiated intensity reported in Dance et al., as inferred from the size of the error bars in the original plots, is about 11%.

3.1. Electrons between 0.5 and 2.0 MeV on aluminum and iron targets

Fig. 1 displays the absolute double-differential distributions (in energy and angle) for the emitted photons in one of the configurations reported by Dance et al., 2.0 MeV electrons on aluminum.

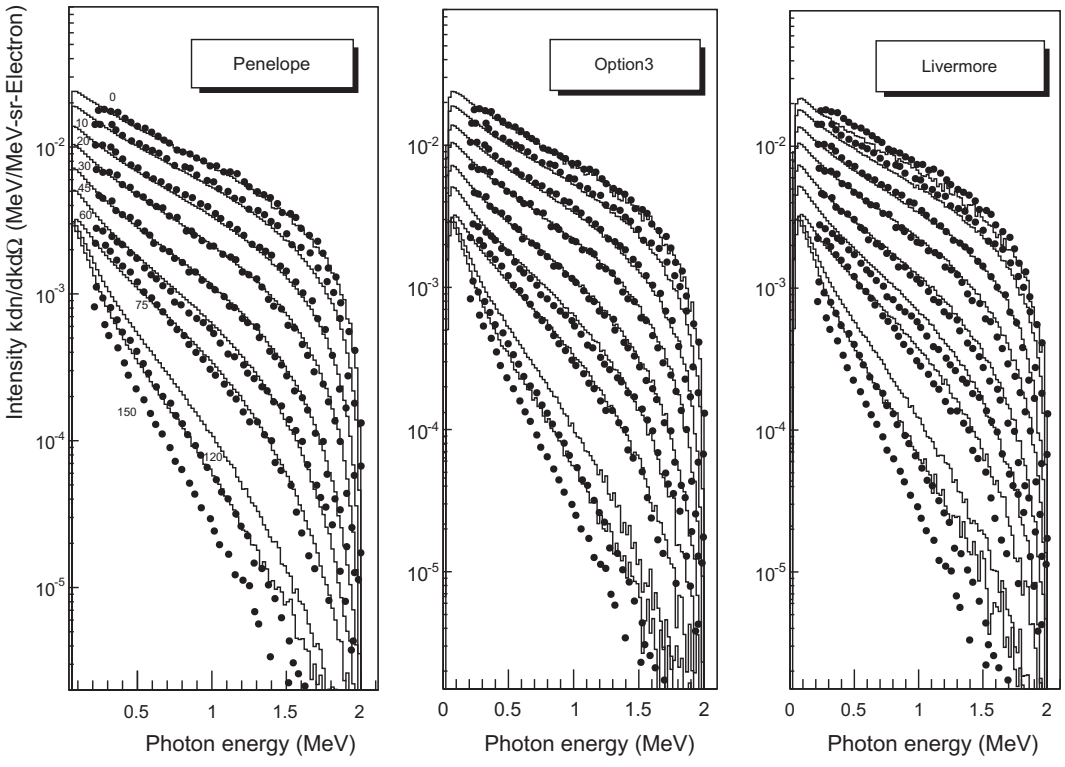

Fig. 1. Absolute energy spectra of photons emitted by 2-MeV electrons impinging on an aluminum target (1.20 g/cm^2) at nine different angles (0°, 10°, 20°, 30°, 45°, 60°, 75°, 120° and 150°). Black circles are experimental data from Dance et al. and solid histogram are the corresponding Monte Carlo simulations. The three sets of models available in GEANT4 are considered.

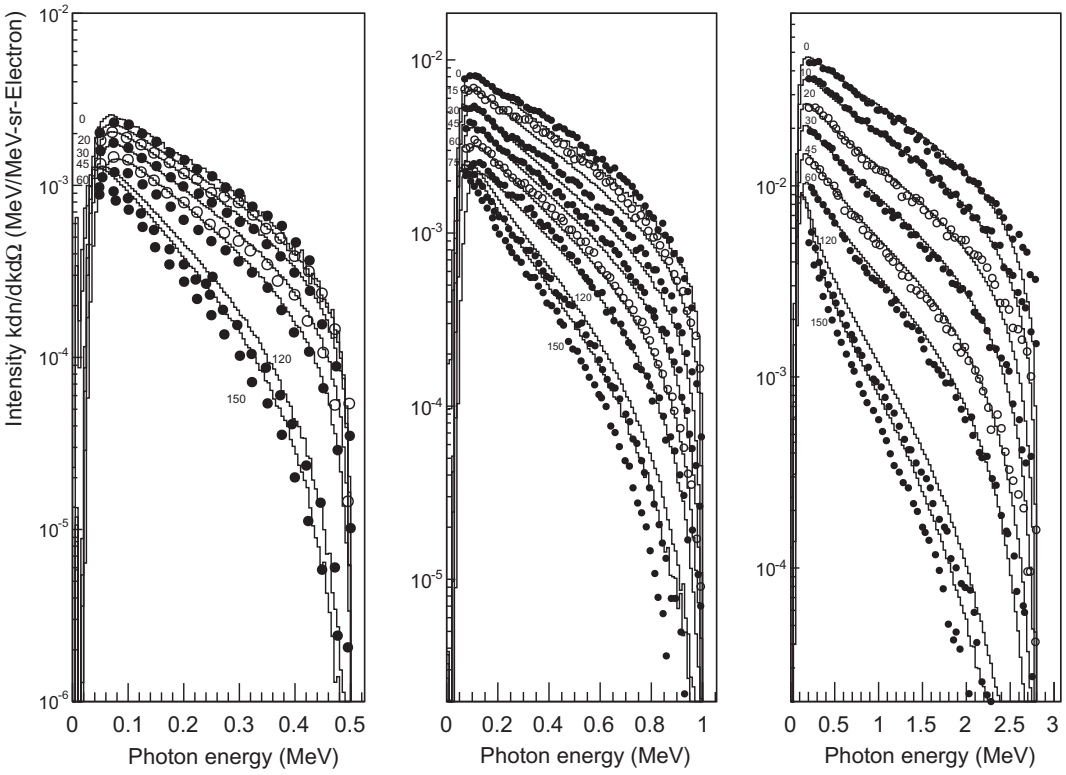

Fig. 2. Absolute energy spectra of photons emitted by electrons of 0.5 MeV (left), 1.0 MeV (middle) and 2.8 MeV (right) on iron targets, at different angles between 0° and 150°. Circles are experimental data from Dance et al. and solid histograms are the GEANT4 simulations obtained with the Penelope model. Some sets of data points are shown as empty circles for visual clarity. The thickness of the targets is 0.257 g/cm^2 (0.5 MeV beam), 0.613 g/cm^2 (1.0 MeV beam) and 2.31 g/cm^2 (2.8 MeV beam).

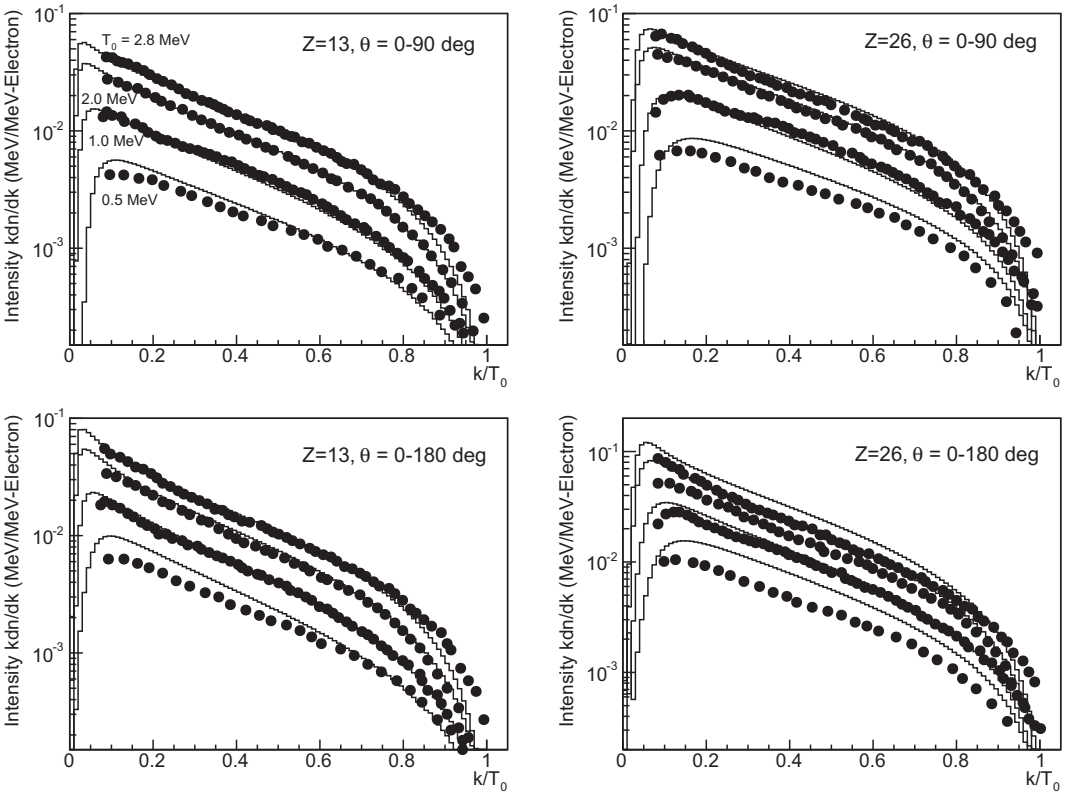

Fig. 3. Absolute energy spectra of photons emitted by electrons of kinetic energy T_0 = 0.5, 1.0, 2.0 and 2.8 MeV on aluminum (left column) and iron (right column) targets. The upper row shows the spectra restricted to forward emission only, and the lower row to the full space. Circles are experimental data from Dance et al. and solid histograms are the GEANT4 simulations obtained with the Penelope model. Photon energy on the *x*-axis is normalized with respect to the kinetic energy of the primary electrons.

Table 1
Total energy radiated in photons, normalized per primary electron, for all the energy-target configurations reported in the paper by Dance et al. The uncertainty of experimental data points is approximately 11% for all configurations. The last three columns summarize the ratio between the photon intensity predicted by the GEANT4 simulation (Option3, Livermore and Penelope models, respectively) and experimental data. The upper half of the table reports the photon yield restricted only to the forward hemisphere, while the lower half reports the all-space yield. The agreement between experimental data and simulations is assessed by a X^2 statistics. The number v of degrees of freedom is also reported.

Material	Energy (MeV)	Data (MeV/electron) (±11%)	Simulation/data		
			Option3	Livermore	Penelope
Forward ($\theta < \pi/2$)					
Al	0.5	$8.80 \cdot 10^{-4}$	0.99	1.00	1.01
Al	1.0	$4.45 \cdot 10^{-3}$	0.70	0.90	0.93
Al	2.0	$1.65 \cdot 10^{-2}$	1.00	1.02	0.99
Al	2.8	$3.52 \cdot 10^{-2}$	0.98	1.00	0.97
Fe	0.5	$1.41 \cdot 10^{-3}$	1.27	1.24	1.23
Fe	1.0	$7.94 \cdot 10^{-3}$	0.83	0.93	0.91
Fe	2.0	$2.99 \cdot 10^{-2}$	0.90	1.04	1.01
Fe	2.8	$6.05 \cdot 10^{-2}$	0.99	1.03	1.00
X^2 ($v = 8$)			18.2	9.8	6.3
All space ($\theta < \pi$)					
Al	0.5	$1.15 \cdot 10^{-3}$	1.16	1.18	1.16
Al	1.0	$5.20 \cdot 10^{-3}$	0.81	1.06	1.08
Al	2.0	$1.78 \cdot 10^{-3}$	1.11	1.15	1.11
Al	2.8	$3.98 \cdot 10^{-2}$	0.99	1.03	0.99
Fe	0.5	$2.08 \cdot 10^{-3}$	1.34	1.37	1.35
Fe	1.0	$1.03 \cdot 10^{-2}$	0.94	1.10	1.08
Fe	2.0	$3.65 \cdot 10^{-2}$	0.99	1.15	1.13
Fe	2.8	$7.52 \cdot 10^{-2}$	1.05	1.09	1.05
X^2 ($v = 8$)			21.9	26.7	19.7
X^2 w/o Fe 0.5 MeV ($v = 7$)			7.9	9.8	5.4

Experimental data are superimposed to the results of the GEANT4 simulations with the three sets of physics models at nine angles between 0° and 150°. All three models predict the correct absolute scale and are able to reproduce the shape of the energy spectra at forward emission angles, which make the leading contribution to the total radiated energy. Nevertheless, all models over-estimate the bremsstrahlung emission in the backward hemisphere and predict a harder energy distribution than measured. The Penelope and Option3 models provide very comparable results and in good agreement with data up to ~75°. The Livermore model provides a very good agreement at intermediate angles, while cannot reproduce data at very small and very large angles. The features described above are observed, at smaller or larger extent, in all configurations of Dance et al., between 0.5 and 2.8 MeV.

The dependence of the double-differential distributions on the electron energy T_0 is displayed in Fig. 2 for the Penelope model: configurations with Fe targets from Dance et al. are considered, with energy between 0.5 and 2.8 MeV. While the general comments above still hold (i.e. correct absolute scale, correct shape of energy spectra at forward angles) it is apparent that the agreement with data gets worse at lower energies. Such a feature is common also to the other physics models. Similarly, all models give results closer to the reference data for lower Z: the agreement with measurements is systematically better in the Al target configurations than in the Fe target.

The same trend is also visible in Fig. 3, which displays the single-differential photon energy spectra obtained with the Penelope model at all electron energies T_0 and in both targets by Dance et al.: Al ($Z = 13$) and Fe ($Z = 26$). Spectra are shown separately for the forward emission hemisphere only (upper row) and for the full space (lower row). A very good agreement is observed for the photons emitted by higher energy electrons and in the forward hemisphere. The agreement is spoiled for lower electron energy and higher Z targets. As discussed above, an over-production of bremsstrahlung photons is observed in the backward hemisphere, which is more evident at lower energy and higher Z.

The paper by Dance et al. also reports (in graphical form) the photon radiated energy vs. the bombarding energy T_0, integrated either over all angles or over the forward hemisphere only. Table 1 summarizes the experimental data I_{meas} and the ratio I_{sim}/I_{meas} between Monte Carlo predictions and data. The uncertainty σ_{meas} of the data points I_{meas} from Dance et al. is about 11% in all configurations. Results for forward emission are very satisfactory: all models agree to data for all eight configurations of Table 1. The Livermore and Penelope predictions are within 10% in all cases, except for Fe at 0.5 MeV (lowest energy at highest Z); the two models are practically equivalent for the aluminum target, while Penelope provides a slightly better agreement with the iron target data. Option3 agrees with data within 30%. Table 1 also reports the X^2 calculated as

$$X^2 = \sum \frac{(I_{meas} - I_{sim})^2}{\sigma^2_{meas}} \quad (1)$$

in order to quantify the global performance of the three sets of models.[3] The Penelope and the Livermore models are both consistent with the data, with the former providing a slightly better agreement. The Option3 model, while giving a very good agreement for the shape of the double-differential spectra, seems to be the least accurate in the prediction on the total energy irradiated in the forward direction.

As expected, results are less good if photons irradiated in the backward direction are also considered. All models fail to reproduce the data point of Fe at 0.5 MeV at more than $3\sigma_{meas}$ and are inconsistent (on average) with the reference data. The single data point of Fe at 0.5 MeV drives the high X^2 values; if this problematic measurement is excluded, all models agree with data within 15–20%. Nevertheless, they show a systematic overestimate of the total radiated energy. The three sets are practically equivalent in the prediction of the all-space yield, with Penelope still providing a bit better agreement with measurements than the others and Option3 being the next.

3.2. 70 keV electrons on aluminum, silver, tungsten and lead targets

The paper from Ambrose et al. reports measurements of photon spectra emitted by 70 keV electrons impinging on thick targets of various materials. The targets are rotated at 45° with respect to the incident beam and they are thick just enough to stop the incident electrons. Photons are detected at emission angles of 45° and 90° with respect to the beam. At the low energy considered by Ambrose et al. the electron ionization process largely dominates and the production of bremsstrahlung photons is relatively scarce.[4] Nevertheless, bremsstrahlung in this energy range is of potential interest for specific medical applications, like imaging and superficial radiotherapy (e.g. for skin lesions).

The validation of GEANT4 with the data at 70 keV has the advantage that bremsstrahlung models are tested in an "unusual"

[3] The X^2 reported here is calculated in the assumption that uncertainties σ_{meas} of the data points are statistical and uncorrelated. No information is reported in Dance et al. about the correlation of experimental errors and about the relative contribution of systematic uncertainties. Therefore, the X^2 should not be regarded here as a χ^2 in its strict statistical meaning, but rather be seen as a parameter to assess the relative performance of the models.

[4] Still, fluorescence X-rays are produced following electron ionization and the characteristic peaks are well visible in the spectra.

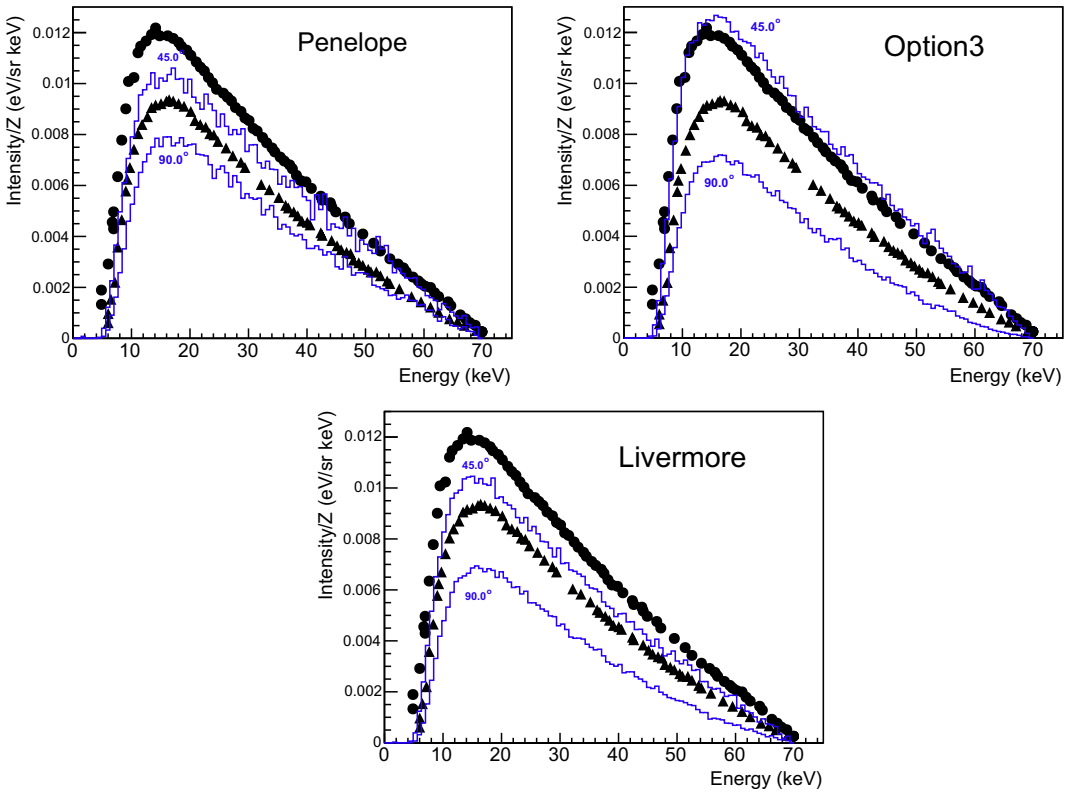

Fig. 4. Absolute energy spectra $\frac{k}{T_0 Z}\frac{dN}{dk d\Omega}$ of photons emitted by 70 keV electrons impinging on a 25.4 mg/cm^2 aluminum target at 45° and 90°. Spectra are normalized according to atomic number Z, solid angle and incident energy T_0. Circles and triangles are experimental data from Ambrose et al. (45° and 90°, respectively). Solid histograms are the GEANT4 simulations obtained with Penelope (upper left), Option3 (upper right) and Livermore (lower left) models.

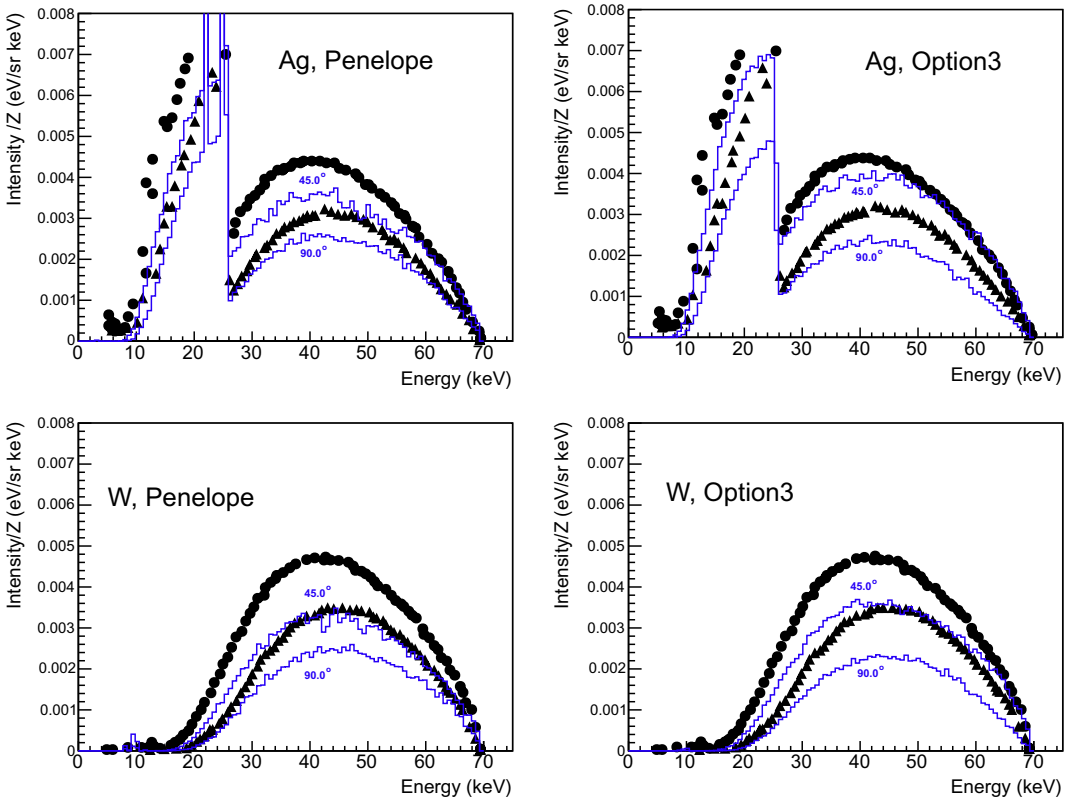

Fig. 5. Absolute energy spectra $\frac{k}{T_0 Z}\frac{dN}{dk d\Omega}$ of photons emitted by 70 keV electrons impinging on silver (28.06 mg/cm^2) and tungsten (50.7 mg/cm^2) targets at 45° and 90°. Spectra are normalized according to atomic number Z, solid angle and incident energy T_0. Circles and triangles are experimental data from Ambrose et al. (45° and 90°, respectively). Solid histograms are the GEANT4 simulations obtained at the two angles with Penelope (left column) and Option3 (right column) models.

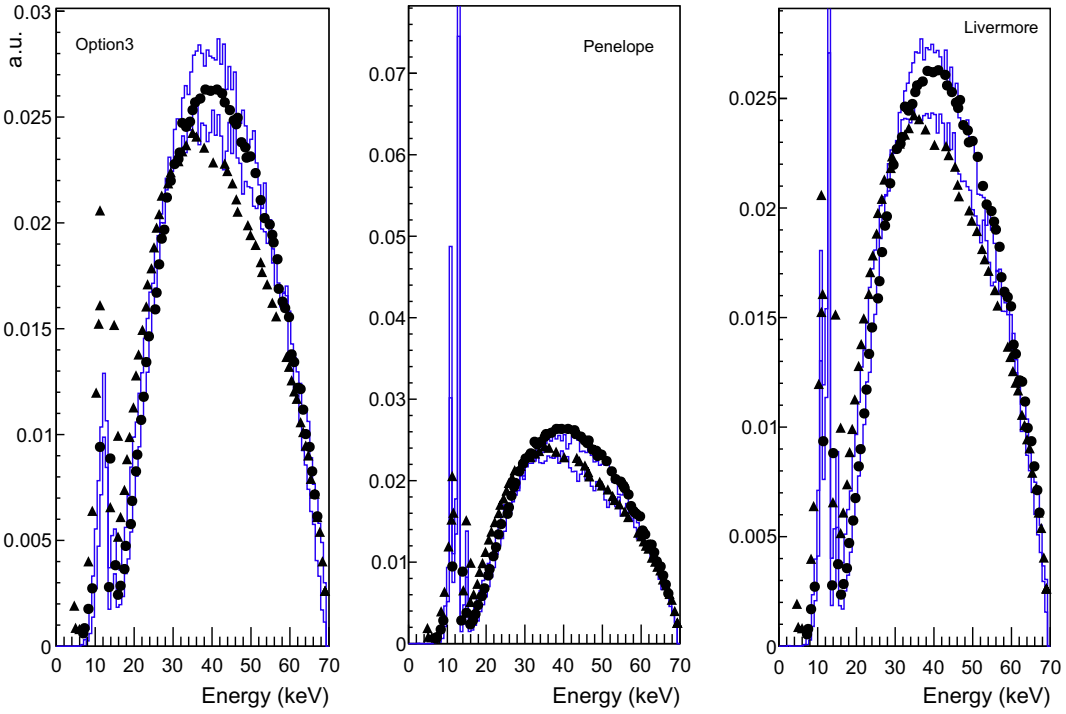

Fig. 6. Qualitative comparison of normalized energy spectra of photons emitted by 70-keV electrons impinging on a 20.89 mg/cm^2 Pb target at 45° and 90°. Circles and triangles are experimental data from Ambrose et al. (45° and 90°, respectively). Solid histograms are the GEANT4 simulations obtained with Option3 (left), Penelope (middle) and Livermore (right) models. Histograms are normalized to match the integrated intensity of the bremsstrahlung continuum (>20 keV) from the experimental data.

energy range, where the process is rare, and experimental measurements are scarce. In fact, bremsstrahlung models are typically developed and tailored for energies above 1 MeV: the capability to reproduce measurements taken at a much different energy cannot be taken for granted a priori and thus provides a confirmation of the validity of the underlying physics modeling. Fig. 4 shows the absolute comparison between experimental data and GEANT4 simulations for both emission angles in the aluminum target, as obtained with the three sets of physics models. All models slightly under-estimate the experimental values, with the exception of the curve obtained at 45° with Option3. Similar conclusions hold for higher-Z targets, as displayed in Fig. 5 (Penelope and Option3 only). Nevertheless, the absolute agreement between data and models concerning the integral photon yield is relatively good: models are able to reproduce the measured photon intensity between 10% and 50%. As observed in Section 3.1, the agreement of simulations with experimental data worsens at higher atomic numbers. When a global scaling factor is applied in order to match the integral intensity of the bremsstrahlung continuum (>20 keV), all models show a good agreement with the measured shape of the photon energy spectra (see Fig. 6). The Livermore and Penelope models provide the best agreement to data.

4. Conclusions

The present work shows that all bremsstrahlung physics models provided by GEANT4 are in reasonable agreement with the experimental data below 3 MeV, both for absolute yields and for spectral shapes. Given the data uncertainties and the lack of a wider set of measurements from different sources, it is hard to provide any deeper assessment of the discrepancies that have been observed. However, a few generic conclusions can be drawn. Good agreement is obtained when forward photon emission is considered, while the agreement is spoiled for back-scattered photons, that are over-estimated both in number and in energy. As a general trend, all physics models show a better agreement with measurements at lower Z values and higher incident electron energies. A good agreement is also observed for the shape of the photon energy spectra emitted by electrons at 70 keV. The total radiated energy is slightly under-estimated by the GEANT4 models, the difference ranging from 10% to 20% in light elements up to 50% in heavy elements. Such a level of precision can be considered as satisfactory in this energy range.

The Penelope model shows the best agreement with measurements for incident electrons energies in the MeV range, but the choice is much less evident at lower energy (below 100 keV). Nevertheless, since in medical physics applications the electron kinetic energies are spread over a wide range, from some keV to tens of MeV, it should be generally preferable to use a physics model able to give an average better response over the range of energies of interest. Consequently, according to our qualitative assessment, the Penelope bremsstrahlung model appears to be slightly preferable with respect to the other two available in GEANT4.

The agreement between GEANT4 simulations and experimental data is found in this work to improve as energy increases. However it is still important to provide a direct validation of the physics models in the energy range of medical applications (3–10 MeV), where experimental data are scarce. Since direct measurements of the spectral distributions are difficult, some authors performed in-phantom measurements of the bremsstrahlung dose by using an electron "raw beam" [35,36]. Additional data in the energy range of 3–10 MeV will eventually give more information to potentially improve the models and consequently the accuracy in the Monte Carlo medical physics applications.

References

[1] B. Faddegon, C. Ross, D. Rogers, Forward-directed bremsstrahlung of 10- to 30-MeV electrons incident on thick targets of Al and Pb, Med. Phys. 17 (1990) 773–785.

[2] I.J. Das, Accelerator beam data commissioning equipment and procedures: report of the TG-106 of the Therapy Physics Committee of the AAPM, Med. Phys. 35 (9) (2008) 4186–4215.

[3] G. Kutcher, L. Coia, M. Gillin, W. Hanson, S. Leibel, R. Morton, J. Palta, J. Purdy, L. Reinstein, G. Svensson, M. Weller, L. Wingfield, Comprehensive QA for radiation oncology: report of AAPM Radiation Therapy Committee Task Group 40, Med. Phys. 21 (1994) 581–618.

[4] E.E. Klein, Task group 142 report: quality assurance of medical accelerators, Med. Phys. 36 (9) (2009) 4197–4212.

[5] H. Koch, J. Motz, Bremsstrahlung cross section formulas and related data, Rev. Mod. Phys. 31 (1959) 920–955.

[6] G. Desobry, A. Boyer, Bremsstrahlung review: an analysis of the Schiff spectrum, Med. Phys. 18 (1991) 497–505.

[7] S. Agostinelli et al., Geant4 – a simulation toolkit, Nucl. Instr. Meth. A 506 (2003) 250–303.

[8] J. Allison et al., Geant4 developments and applications, IEEE Trans. Nucl. Sci. 53 (2006) 270–278.

[9] J. Baró, J. Sempau, J. Fernández-Varea, F. Salvat, PENELOPE: an algorithm for Monte Carlo simulation of the penetration and energy loss of electrons and positrons in matter, Nucl. Instr. Meth. B 100 (1995) 31–46.

[10] I. Kawrakow, Accurate condensed history Monte Carlo simulation of electron transport. I. EGSnrc, the new EGS4 version, Med. Phys. 27 (2000) 485–498.

[11] G. Battistoni et al., The FLUKA code: description and benchmarking, AIP Conf. Proc. 896 (2007) 31–49.

[12] A. Ferrari, P. Sala, A. Fassò, J. Ranft, FLUKA: a multi-particle transport code. 2005, http://dx.doi.org/10.5170/CERN-2005-010.

[13] B. Faddegon et al., Benchmarking of Monte Carlo simulation of bremsstrahlung from thick targets at radiotherapy energies, Med. Phys. 35 (2008) 4308–4317.

[14] W. Dance et al., Bremsstrahlung produced in thick aluminum and iron targets by 0.5 to 2.8 MeV electrons, J. Appl. Phys. 39 (1968) 2881–2889.

[15] R. Ambrose, D. Kahler, H. Lehtihet, C. Quarles, Angular dependence of thick-target bremsstrahlung, Nucl. Instr. Meth. B 56 (57) (1991) 327–329.

[16] G. Weidenspointner, M. Batic, S. Hauf, G. Hoff, M. Kuster, M. Pia, P. Saracco, Validation of Compton scattering Monte Carlo simulation models, to be published in the Proceedings of IEEE Nuclear Science Symposium 2013 (2014). arXiv:1401.1660.

[17] M. Begalli, G. Hoff, M. Pia, P. Saracco, Validation of Geant4 Electron Pair Production by Photons, to be published in the Proceedings of IEEE Nuclear Science Symposium 2013 (2013). arXiv:1311.5155.

[18] T. Basaglia, M. Batic, M.C. Han, G. Hoff, C. Kim, H. Kim, M. Pia, P. Saracco, Physics Methods for the Simulation of Photoionisation, to be published in the Proceedings of IEEE Nuclear Science Symposium 2013 (2013). arXiv:1311.5153.

[19] M. Batic, G. Hoff, M. Pia, P. Saracco, G. Weidenspointner, Validation of Geant4 simulation of electron energy deposition, IEEE Trans. Nucl. Sci. 60 (2013) 2934–2957.

[20] J. Apostolakis et al., Geometry and physics of the Geant4 toolkit for high and medium energy applications, Rad. Phys. Chem. 78 (2009) 859–873.

[21] V. Ivanchenko et al., Recent improvements in Geant4 electromagnetic physics models and interfaces, Prog. Nucl. Sci. Technol. 2 (2011) 898–903.

[22] V. Ivanchenko et al., Geant4 electromagnetic physics: improving simulation performance and accuracy, Proceedings of SNA + MC 2013 (2014) 03101.

[23] J. Allison et al., Geant4 electromagnetic physics for high statistic simulation of LHC experiments, J. Phys. Conf. Ser. 396 (2012) 022013.

[24] S. Chauvie et al., Geant4 low energy electromagnetic physics, IEEE Nucl. Sci. Symp. Conf. Record 3 (2004) 1881–1885.

[25] S. Seltzer, M. Berger, Bremsstrahlung spectra from electron interactions with screened atomic nuclei and orbital electrons, Nucl. Instr. Meth. B 12 (1985) 95–134.

[26] S. Seltzer, M. Berger, Bremsstrahlung energy spectra from electrons with kinetic energy 1 keV – 10 GeV incident on screened nuclei and orbital electrons of neutral atoms with Z = 1–100, At. Data Nucl. Data Table 35 (1986) 345–418.

[27] Y.-S. Tsai, Pair production and bremsstrahlung of charged leptons, Rev. Mod. Phys. 46 (1974) 815–851.

[28] Y.-S. Tsai, Erratum: pair production and bremsstrahlung of charged leptons, Rev. Mod. Phys. 49 (1977) 421–423.

[29] Geant4 Collaboration, Geant4 Physics Reference Manual. 2013.

[30] S. Perkins, D. Cullen, S. Seltzer, Tables and graphs of electron-interaction cross-sections from 10 eV to 100 GeV Derived from the LLNL Evaluated Electron Data Library (EEDL), Z=1-100, Report UCRL-50400, vol. 31, 1991.

[31] A. Bielajew, R. Mohan, C.-S. Chui, Improved bremsstrahlung photon angular sampling in the EGS4 code system, report NRCC/PIRS-0203 (1989).

[32] J. Sempau, J. Fernández-Varea, E. Acosta, F. Salvat, Experimental benchmarks of the Monte Carlo code PENELOPE, Nucl. Instr. Meth. B 207 (2003) 107–123.

[33] F. Salvat, J. Fernández-Varea, J. Sempau, PENELOPE, a code system for Monte Carlo simulation of electron and photon transport, report NEA-6416 (2009).

[34] L. Kissel et al., Shape functions for atomic-field bremsstrahlung from electrons of kinetic energy 1–500 keV on selected neutral atoms $1 \leqslant Z \leqslant 92$, At. Data Nucl. Data Table 28 (1983) 381–460.

[35] D. Sawkey, B. Faddegon, Comparison of beam characteristics of a gold X-ray target and a tungsten replacement target, Med. Phys. 36 (2009) 5622–5632.

[36] D. Sawkey et al., A diamond target for megavoltage cone-beam CT, Med. Phys. 37 (2010) 1246–1253.